Observations of electronic inhomogeneity in heavily Pb-doped $Bi_2Sr_2CaCu_2O_y$ single crystals by scanning tunneling microscopy

G. Kinoda* and T. Hasegawa
Frontier Collaborative Research Center, Tokyo Institute of Technology, 4259 Nagatsuta-cho, Midori-ku, Yokohama 226-8503, Japan

S. Nakao, T. Hanaguri,† K. Kitazawa,† K. Shimizu, J. Shimoyama,† and K. Kishio†
Department of Superconductivity, University of Tokyo, 7-3-1 Hongo, Bunkyo-ku, Tokyo 113-8656, Japan
(Received 27 January 2003; revised manuscript received 18 March 2003; published 17 June 2003)

Cleaved ab surfaces of heavily Pb-doped $Bi_2Sr_2CaCu_2O_y$ single crystals, including phase separation into Pb-poor α and Pb-rich β phases, were probed by cryogenic scanning tunneling microscopy/spectroscopy at 4.3 K. We could resolve individual Pb atoms substituted into Bi sites, which tend to be concentrated on the crest of modulation in the α phase, but are almost randomly dispersed throughout the β phase. The scanning tunneling spectroscopy results revealed a considerably wide range of gap values Δ, originating from the presence of both superconducting and pseudogap regions on a nanometer scale. Furthermore, we found that oxygen annealing substantially increases gap inhomogeneity. This strongly suggests that disorder of excess oxygen, possibly coupled with structural deformation of CuO_2 sheets, destroys superconducting coherence, resulting in the appearance of a pseudogap.

DOI: 10.1103/PhysRevB.67.224509 PACS number(s): 74.25.Jb, 74.62.Dh, 74.72.−h, 87.64.Dz

Scanning tunneling microscopy/spectroscopy (STM/STS) is now widely recognized as a tool for directly probing spatial distributions of local density of states (LDOS) at an atomic scale. This technique has been extensively used to investigate low-energy excitation spectra in high-T_c superconductors (HTSC's) with nanometer-scale structural features, such as impurity atoms[1,2] and vortex cores,[3–5] in order to elucidate their pairing mechanisms.

Other recent STM/STS investigations into local properties of HTSC's have revealed inherent inhomogeneity in superconducting states, mainly observed in optimally[6] and underdoped $Bi_2Sr_2CaCu_2O_y$ (Bi2212) (Refs. 7–10) single crystals. In particular, in underdoped Bi2212,[10] granular superconductivity on a ~3 nm scale has been observed, a phenomenon in which superconducting domains with well-developed *d*-wave gaps are finely dispersed throughout a dominant nonsuperconducting matrix that exibits pseudogaplike spectra. It has also been shown that such a phenomenon is not a consequence of impurity atoms introduced into the CuO_2 layer.[6,10] To date, many possible causes of this microscopic inhomogeneity have been proposed, including nonuniformly distributed pair breakers or carriers,[11] unscreened ionic potentials,[6,12,13] and atomic scale disorders.[7,14,15] In contrast, overdoped HTSC's are generally believed to exhibit pure *d*-wave states, and suffer less from electronic inhomogeneity. Indeed, the pseudogap disappears in a macroscopic sense, as asserted by photoemission measurements.[16–18] Therefore local properties of overdoped Bi2212 that can be directly probed by microscopic techniques manifest intrinsic material parameters that govern the spatial variation of superconducting states in a more discernible manner.

Here, we report the results of cryogenic STM/STS of Pb-doped $Bi_{2-x}Pb_xSr_2CaCu_2O_y$ (Pb-Bi2212) single crystals with $x=0.6$, in which substitution of divalent Pb for trivalent Bi introduces carriers into the CuO_2 plane, resulting in heavily overdoped crystals. STM images reveal a lamellalike structure indicating a phase separation into Pb-poor and Pb-rich domains. STS results confirm the existence of electronic

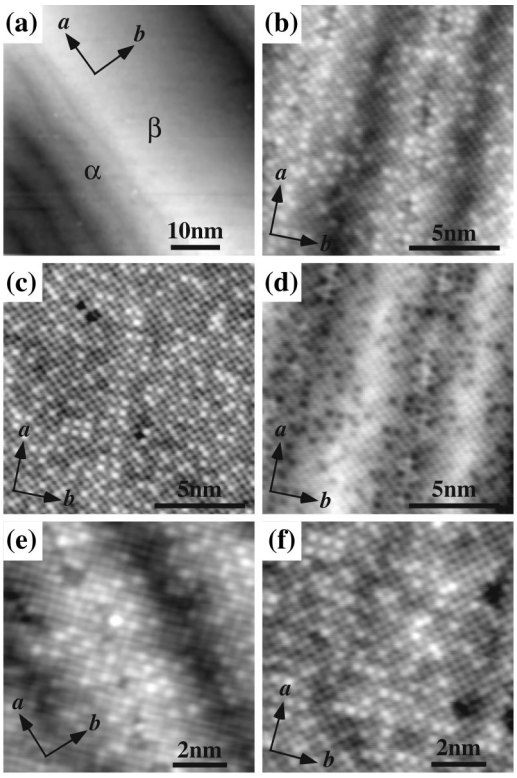

FIG. 1. STM images of Pb-Bi2212 single crystals at 4.3 K. (a) Wide scan picture showing both α and β phases; (b) α phase and (c) β phase images of an as-grown sample; (d) inverted contrast image of (b); (e) α phase and (f) β phase images of an annealed sample. A contrast along the b axis in (a) is mainly due to topography. Tunneling conditions were (a) $V_s=490$ mV, $I_t=0.3$ nA, (b) $V_s=320$ mV, $I_t=0.4$ nA, (c) $V_s=800$ mV, $I_t=0.4$ nA, (e) $V_s=100$ mV, $I_t=0.7$ nA, (f) $V_s=100$ mV, $I_t=0.6$ nA.

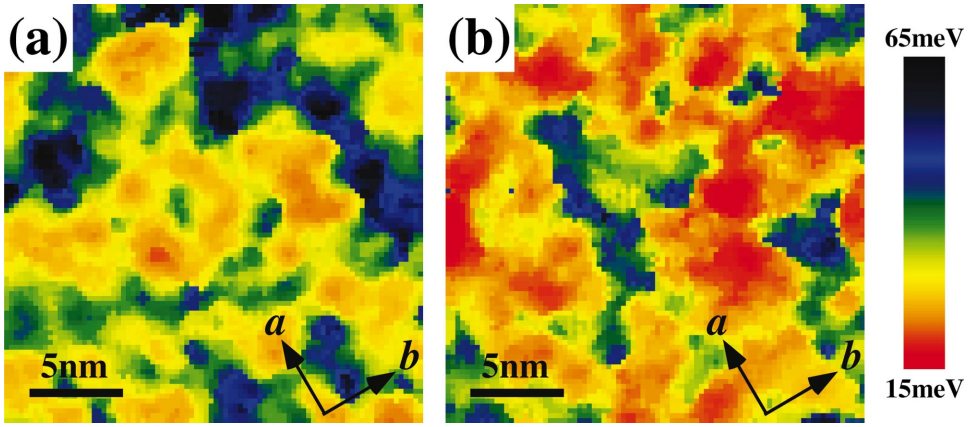

FIG. 2. (Color) Δ maps of (a) α and (b) β phases observed on an annealed Pb-Bi2212 single crystal at 4.3 K. Tunneling conditions were (a) $V_s = 100$ mV, $I_t = 0.7$ nA, and (b) $V_s = 100$ mV, $I_t = 0.4$ nA.

inhomogeneity over nanometer scales, with details of the inhomogeneity, depending on local domain Pb content x and degree of annealing. Based on statistical analysis of gap distribution, we discuss origins of the local pseudogap state.

Pb-Bi2212 single crystals with $x = 0.6$ were grown using the floating zone technique. Details of the crystal-growth procedure have been described elsewhere.[19] As-grown crystals were post-annealed in a pure oxygen atmosphere of $P(O_2) = 2.1$ atm at 400 °C for 3 days. Superconducting transition temperatures T_c of as-grown and annealed crystals were found to be 82 and 68 K, respectively, using a superconducting quantum interference device susceptometer.

STM/STS measurements were carried out using a home-built UHV-LT-STM equipped with a low-temperature cleavage mechanism.[20] The base pressure of the STM chamber was maintained at less than 2.0×10^{-10} Torr during measurements. All Pb-Bi2212 samples examined here were cleaved *in situ* at 77 K, then immediately transferred to the STM head under refrigerated conditions in order to minimize oxygen loss from sample surfaces. Mechanically sharpened Pr-Ir alloy STM tips were used.

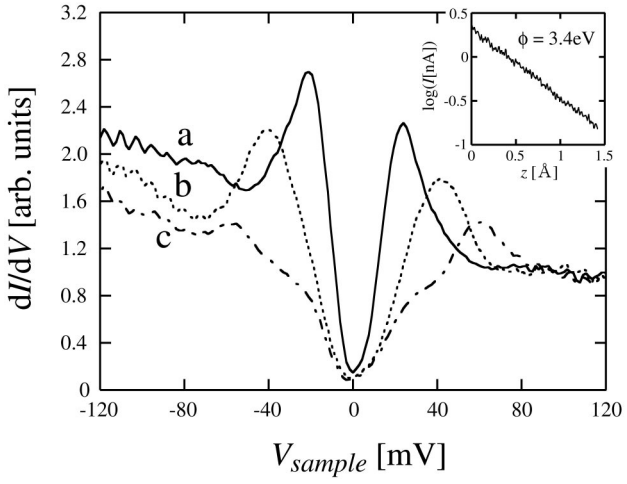

FIG. 3. Tunneling spectra averaged over (a) smaller ($\Delta < 30$ meV), (b) intermediate (30 meV$< \Delta < 50$ meV), and (c) larger ($\Delta > 50$ meV) Δ regions in Fig. 2(a). The spectra are normalized to 100 mV. A typical z-log(I) curve is plotted in the inset.

Figure 1 shows a set of STM images taken of cleaved ab surfaces of as-grown and annealed Pb-Bi2212 crystals at 4.3 K. Figure 1(a) shows a wide scan image, demonstrating the lamellalike phase separation into modulated (α phase) and modulation-free (β phase) regions, analogous to those reported by previous TEM (Ref. 21) and STM observations.[22,23] Even in the α phase, a modulation periodicity of ~6 nm was observed, much longer than that of undoped Bi2212, indicating that both phases were in the heavily overdoped regime. Most of strong contrast along the b axis seen in Fig. 1(a) is due to topography. Figures 1(b) and 1(c) are narrower scan images taken of the α and β phase regions, respectively, of an as-grown crystal, in which square lattices of Bi atoms are clearly resolved. In the figures, it is notable that some atomic sites are brighter than others, i.e., have larger corrugation. These brighter spots are more prevalent in the β phase ($24 \pm 1\%$ of Bi sites) than in the α phase ($20 \pm 2\%$). Therefore we identify the spots as Pb atoms substituted into Bi sites. These Pb contents are in good agreement with the analyzed values by ICP, $x \sim 0.4$.[19] In the present study, we have reproducibly observed regularly arranged square lattice patterns, as shown in Fig. 1, but did not see any

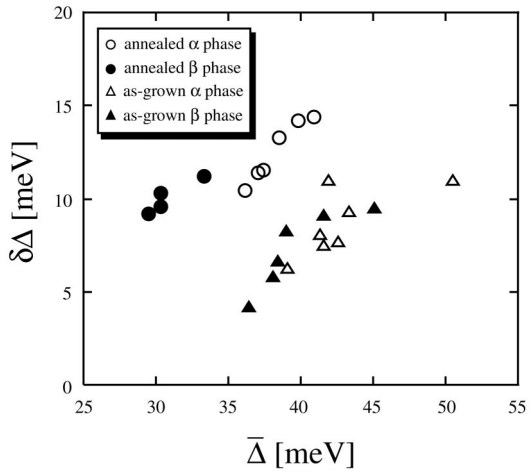

FIG. 4. Plots of $\delta\Delta$ against-$\bar{\Delta}$ for α and β phase regions in as-grown and annealed samples with several different Pb content fractions.

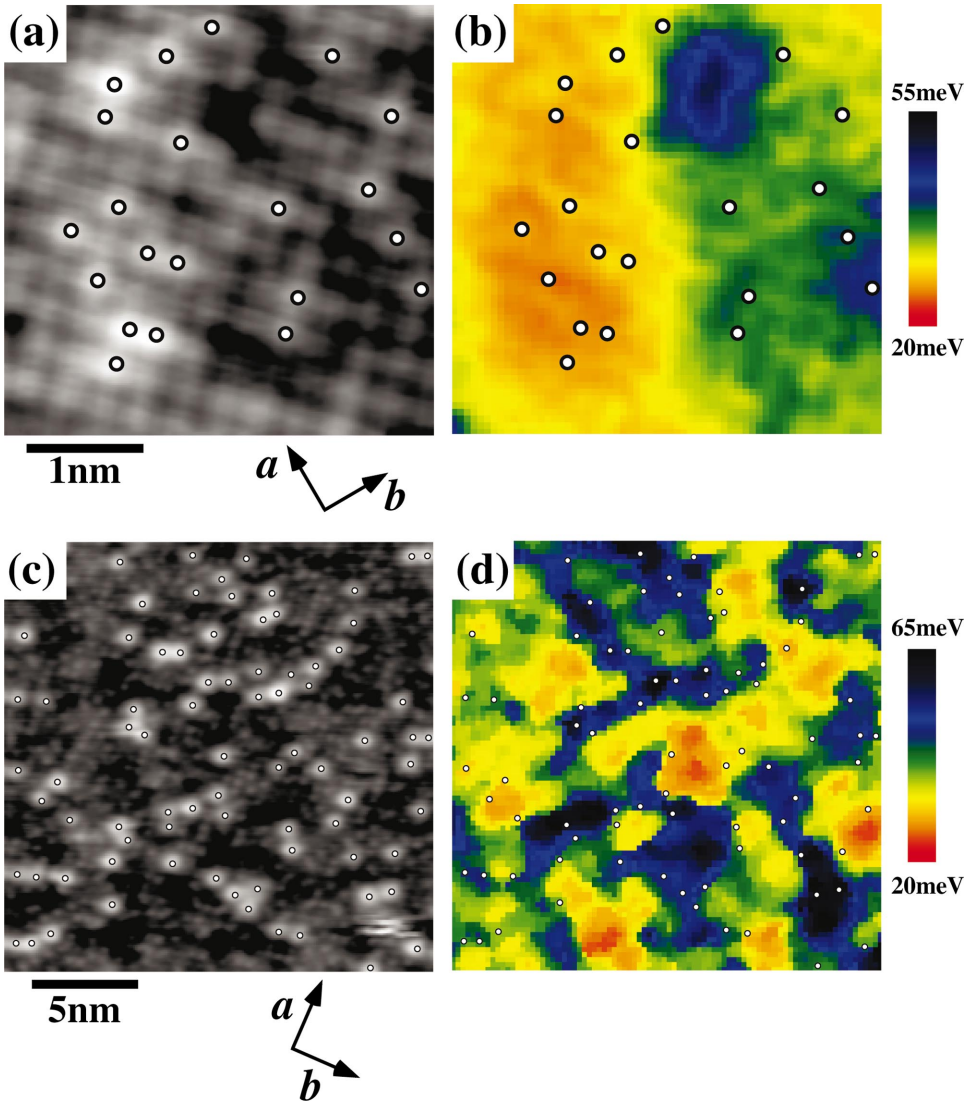

FIG. 5. (Color) Correlations between impurity distributions and Δ maps in Pb-Bi2212 at 4.3 K. (a) STM image resolving Pb atoms and (b) corresponding Δ map obtained in an annealed sample. (c) STM image resolving Sr(Ca)-site defects and (d) corresponding Δ map obtained in an as-grown sample. The tunneling conditions were (a), (b) $V_s = 0.1$ V and $I_t = 0.5$ nA, (c) $V_s = 1.8$ V and $I_t = 0.3$ nA, and (d) $V_s = 0.1$ V and $I_t = 0.4$ nA.

sign of disorder, as suggested by Cren *et al.*[8]

Figure 1(d) shows the image of Fig. 1(b) with the contrast inverted, so that Pb atoms located in the trough of modulation can be easily distinguished as dark spots. By comparison of the two figures, it is evident that Pb atoms are not homogeneously dispersed throughout the BiO layer, but favor locations in the crest of the modulation. In other words, Pb atoms are concentrated in locations where the distance between adjacent BiO layers is minimal. In contrast, Pb atoms in the β phase seem to be distributed randomly, as seen in Fig. 1(c). Figures 1(e) and (f) show images of α and β phases in annealed crystal. Here, we emphasize that Pb distribution patterns are not significantly altered by annealing in oxygen at a relatively low temperature, 400 °C. The Pb content differs from one domain to another, being in the ranges of $18 \pm 1\%$ and $23 \pm 3\%$ in the α and β phases, respectively, almost identical to those observed in as-grown crystals.

We have also performed STS measurements of both as-grown and annealed samples at 4.3 K. Figure 2 shows a map of local gap values Δ for α and β phases of an annealed sample. Values of Δ were deduced from conductance spectra as the half the peak-to-peak energy separation. In both α and β phases, Δ is spatially nonuniform over a length scale of 2–6 nm, similar to previous STM observations of optimally[6] and underdoped Bi2212,[7–10] and exhibits a broad distribution of gap values, from 20 to 65 meV and from 15 to 60 meV for the α and β phases, respectively. This implies that electronic inhomogeneity is general property of Bi2212, and its existence is not dependent on carrier concentration.

Tunneling spectra, averaged over small ($\Delta < 30$ meV), intermediate (30 meV $< \Delta < 50$ meV), and large ($\Delta > 50$ meV) Δ regions, are plotted in Fig. 3. The tunneling barrier height ϕ was checked before and after STS measurement, as shown in the inset of Fig. 3, to make sure it was sufficiently high, ~3 eV. This ensures us ideal vacuum tunneling conditions during measurement. The spectrum repre-

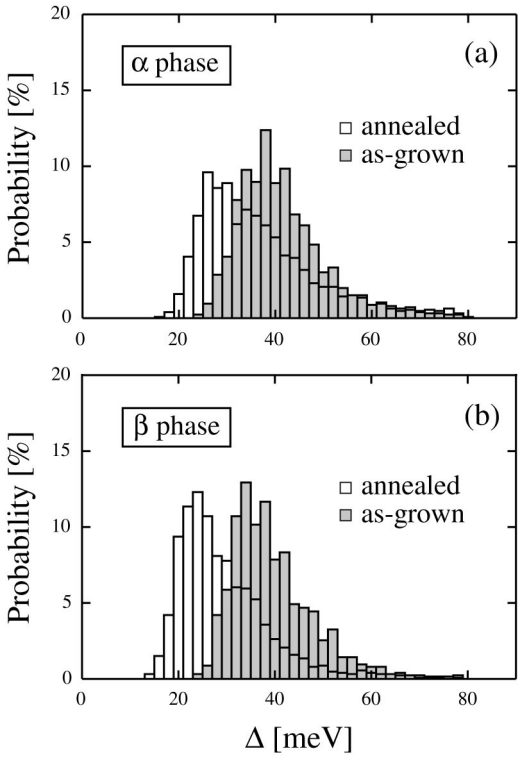

FIG. 6. Δ distributions of (a) α and (b) β phase regions of as-grown and annealed samples.

senting low Δ is characterized by a clear superconducting gap, well-developed coherence peaks, and an overall asymmetry.[24] In the large Δ region, on the contrary, we found pseudogaplike behavior distinguished by significantly suppressed conductance peaks.[6–10] One can also recognize a so-called dip-hump structure adjacent to the coherence peaks in the ''superconducting'' spectrum, but the structure is considerably suppressed in the pseudogaplike regions. These features are in qualitative agreement with the previous reports on Pb-Bi2212 by Cren *et al.*,[8] although the dip-hump structure in Fig. 3 is relatively weaker, possibly reflecting that our crystals are more overdoped.[25]

Next, we examine electronic inhomogeneity more quantitatively, using statistical analyses of Δ distributions as a basis. Figure 4 shows average and root-mean-square values of Δ, represented by $\overline{\Delta}$ and $\delta\Delta$ respectively, calculated from several α and β domains with different Pb contents. There is a positive correlation between $\overline{\Delta}$ and $\delta\Delta$ in both as-grown and annealed sample series. That is, the gap inhomogeneity $\delta\Delta$ is suppressed by a decrease in $\overline{\Delta}$, which is caused by an increase in Pb content *x*. These results clearly prove that the Pb content does affect the inhomogeneity, but the randomness of it does not. We have also confirmed that Pb distributions, as measured by STM, do not correlate with corresponding Δ patterns. Figure 5(a) is a high-resolution STM image measured at 4.3 K, resolving several Pb atoms. Figure 5(b) is a corresponding spatial map of Δ values. In both images, the locations of Pb atoms are marked by open circles. Comparing two images, it is evident that the Pb distribution is not attributable to the Δ inhomogeneity. The low-temperature STM/STS observations of Pb-Bi2212 by Cren *et al.*[8] reported that superconducting domains exist within regions of peakless gap structure, which were referred to as low-temperature pseudogap (LTPG) regions. By comparing LDOS maps to theoretical predictions, they concluded that the transition from superconducting gap to LTPG is attributable to disorders induced by Bi/Pb substitution. However, our atomic-resolution STS results unambiguously rule out such a possibility.

Figures 5(c) and (d) show an STM image, taken at a high bias voltage of 1.8 V, and a corresponding Δ map, respectively. As seen in Fig. 5(c), we find new bright spots, which appear for the biases $V_s > 1.4$ V. It is also confirmed that each bright spots are located at the center of a square surrounded by four adjacent Bi(Pb) atoms. Considering from the crystal structure of Pb-Bi2212, we tentatively assign the bright spots as natural impurities or defects occupying Sr or Ca sites. The open circles drawn in Figs. 5(c) and (d) indicate the locations of Sr(Ca)-site defects. Again, there is no correlation between the distribution of Sr(Ca)-site defects and the Δ pattern. Furthermore, we also found natural defects at Cu sites, which cause quasiparticle scattering.[1,2,10] However, their number density is estimated to be 0.05–0.08% of Cu, which is negligibly small compared with the volume fraction of pseudogap regions. These facts strongly suggest that excess oxygen disorders in the $(BiO)_2$ layers, which are invisible to STM, destroy superconducting phase coherence and give rise to local pseudogap states, which is consistent with the STM/STS results for pure Bi2212 reported by Pan *et al.*[6]

In contrast to the Pb doping, oxygen annealing was found to significantly shift the $\overline{\Delta}$-$\delta\Delta$ plot upward, i.e., increase $\delta\Delta$. To understand the effect of annealing on $\delta\Delta$ in more detail, individual Δ distributions, as plotted in Fig. 4, were categorized into four groups in terms of phase and annealing conditions. Δ histograms for each group are compared in Fig. 6. Oxygen annealing considerably reduces the minimum value of Δ, but has less of an impact on the number of domains with larger $\overline{\Delta}$, resulting in broadening of the Δ histogram. This implies that although carriers associated with oxygen annealing can reduce the superconducting gap, pseudogaplike domains are not easily transformed into superconducting domains. This is in sharp contrast to the case of Pb substitution, which causes an almost constant shift of Δ histogram to lower energies. Since Pb substitution tends to reduce excess oxygen,[19] the decrease in $\delta\Delta$ with *x*, shown in Fig. 4, is consistent with the described local picture assuming disorder-driven inhomogeneity. Moreover, as seen in Fig. 6(a), pseudogaplike states with $\Delta > 50$ meV in the α phase are mainly unaffected by annealing. Since α phase exhibits modulation along the *b* axis, which affects CuO_2-CuO_2 distances, it is likely that the structural deformations of CuO_2 sheets pin oxygen disorders to van der Waals sites, thus stabilizing the pseudogap.

In summary, we have performed cryogenic STM/STS observations of Pb-doped Bi2212 single crystals in order to investigate local electronic structures in the heavily overdoped regime. STM/STS results clearly show electronic inhomogeneities across a nanometer scale composed of super-

conducting and pseudogaplike regions. The Δ distribution tends to narrow with increasing Pb content, giving clear evidence that Pb atoms substituted into Bi sites are not responsible for inhomogeneity. On the other hand, oxygen annealing at a relatively low temperature, 400 °C, broadens the Δ distribution. As a consequence, it is proposed that pseudogaplike states originate from disorders of excess oxygen, which may become stable when coupled with CuO_2 sheet structural deformations.

Two of the authors (G.K. and S.N.) were supported in carrying out this work by the Japan Society for Promotion of Science (JSPS).

*Electronic address: kinoda@nano.fcrc.titech.ac.jp
†Also at SORST, Japan Science and Technology Corporation.

[1] S. H. Pan, E. W. Hudson, K. M. Lang, H. Eisaki, S. Uchida, and J. C. Davis, Nature (London) **403**, 746 (2000).
[2] W. E. Hudson, K. M. Lang, V. Madhavan, S. H. Pan, H. Eisaki, S. Uchida, and J. C. Davis, Nature (London) **411**, 920 (2001).
[3] I. Maggio-Aprile, Ch. Renner, A. Erb, E. Walker, and Ø. Fischer, Phys. Rev. Lett. **75**, 2754 (1995).
[4] Ch. Renner, B. Revaz, K. Kadowaki, I. Maggio-Aprile, and Ø. Fischer, Phys. Rev. Lett. **80**, 3606 (1998).
[5] S. H. Pan, E. W. Hudson, A. K. Gupta, K.-W. Ng, H. Eisaki, S. Uchida, and J. C. Davis, Phys. Rev. Lett. **85**, 1536 (2000).
[6] S. H. Pan, J. P. O'Neal, R. L. Badzey, C. Chamon, H. Ding, J. R. Engelbrecht, Z. Wang, H. Eisaki, S. Uchida, A. K. Gupta, K.-W. Ng, E. W. Hudson, K. M. Lang, and J. C. Davis, Nature (London) **413**, 282 (2001).
[7] T. Cren, D. Roditchev, W. Sacks, J. Klein, J.-B. Moussy, C. Deville-Cavellin, and M. Laguës, Phys. Rev. Lett. **84**, 147 (2000).
[8] T. Cren, D. Roditchev, W. Sacks, and J. Klein, Europhys. Lett. **54**, 84 (2001).
[9] C. Howald, P. Fournier, and A. Kapitulnik, Phys. Rev. B **64**, 100504(R) (2001).
[10] K. M. Lang, V. Madhavan, J. E. Hoffman, E. W. Hudson, H. Eisaki, S. Uchida, and J. C. Davis, Nature (London) **415**, 412 (2002).
[11] Y. N. Ovchinnikov, S. A. Wolf, and V. Z. Kresin, Phys. Rev. B **63**, 064524 (2001).
[12] Q.-H. Wang, J. H. Han, and D.-H. Lee, Phys. Rev. B **65**, 054501 (2001).
[13] Z. Wang, J. R. Engelbrecht, S. Wang, H. Ding, and S. H. Pan, Phys. Rev. B **65**, 064509 (2002).
[14] C. Huscroft and R. T. Scalettar, Phys. Rev. Lett. **81**, 2775 (1998).
[15] J. Burgy, M. Mayr, V. Martin-Mayor, A. Moreo, and E. Dagotto, Phys. Rev. Lett. **87**, 277202 (2001).
[16] A. G. Loser, Z.-X. Shen, D. S. Dessau, D. S. Marshall, C. H. Park, P. Fournier, and A. Kapitulnik, Nature (London) **273**, 325 (1996).
[17] H. Ding, T. Yokoya, J. C. Campuzano, T. Takahashi, M. Randeria, M. R. Norman, T. Mochiku, K. Kadowaki, and J. Giapintzakis, Nature (London) **382**, 51 (1996).
[18] M. R. Norman, H. Ding, M. Randeria, J. C. Campuzano, T. Yokoya, T. Takeuchi, T. Takahashi, T. Mochiku, K. Kadowaki, P. Guptasarma, and D. G. Hinks, Science **392**, 157 (1998).
[19] T. Motohashi, Y. Nakayama, T. Fujita, K. Kitazawa, J. Shimoyama, and K. Kishio, Phys. Rev. B **59**, 14080 (1999).
[20] G. Kinoda, T. Yamanouchi, H. Suzuki, T. Endo, K. Kitazawa, and T. Hasegawa, Physica C **353**, 297 (2001).
[21] I. Chong, Z. Hiroi, J. Shimoyama, Y. Nakayama, K. Kishio, T. Terashima, Y. Bando, and M. Takano, Science **276**, 770 (1997).
[22] S. Nakao, K. Ueno, T. Hanaguri, K. Kitazawa, T. Fujita, Y. Nakayama, T. Motohashi, J. Shimoyama, K. Kishio, and T. Hasegawa, J. Low Temp. Phys. **117**, 341 (1999).
[23] M. Nishiyama, K. Ogawa, I. Chong, Z. Hiroi, and M. Takano, Physica C **314**, 229 (1999).
[24] Ch. Renner and Ø. Fischer, Phys. Rev. B **51**, 9208 (1995).
[25] Ch. Renner, B. Revaz, J.-Y. Genoud, K. Kadowaki, and Ø. Fischer, Phys. Rev. Lett. **80**, 149 (1998).